Available online at www.sciencedirect.com

ScienceDirect

Journal of Nutritional Biochemistry 25 (2014) 496–502

Journal of Nutritional Biochemistry

Folic acid stimulation of neural stem cell proliferation is associated with altered methylation profile of PI3K/Akt/CREB☆,☆☆

Min Yu[a,1], Wen Li[a,1], Suhui Luo[a], Yan Zhang[b], Huan Liu[a], Yuxia Gao[c], Xuan Wang[a], John X. Wilson[d], Guowei Huang[a,*]

[a]Department of Nutrition and Food Science, School of Public Health, Tianjin Medical University, Tianjin 300070, China
[b]School of Bioinformatics Science and Technology, Harbin Medical University, Harbin 150081, China
[c]Department of Cardiology, General Hospital of Tianjin Medical University, Tianjin 300052, China
[d]Department of Exercise and Nutrition Sciences, School of Public Health and Health Professions, University at Buffalo, Buffalo, NY 14214–8028, USA

Received 12 August 2013; received in revised form 13 December 2013; accepted 30 December 2013

Abstract

Proliferation of neural stem cells (NSCs) is required for development and repair in the nervous system. NSC amplification *in vitro* is a necessary step towards using NSC transplantation therapy to treat neurodegenerative diseases. Folic acid (FA) has been shown to act through DNA methyltransferase to stimulate NSC proliferation. To elucidate the underlying mechanism, the effect of FA on the methylation profiles in neonatal rat NSCs was assessed by methylated DNA immunoprecipitation (MeDIP) and methylated DNA immunoprecipitation-DNA microarray (MeDIP-Chip). Differentially methylated regions (DMRs) were determined by quantitative differentially methylated regions analysis, and genes carrying at least three DMRs were selected for pathway analysis. Gene network analysis revealed links with steroid biosynthesis, fatty acid elongation and the PI3K/Akt/CREB, neuroactive ligand–receptor interaction, Jak-STAT and MAPK signaling pathways. Moreover, Akt3 acted as a hub in the network, in which 14 differentially methylated genes converged to the PI3K/Akt/CREB signaling pathway. These findings indicate that FA stimulates NSC proliferation by modifying DNA methylation levels in the PI3K/Akt/CREB pathway.

Keywords: Folic acid; DNA methylation; Neural stem cells; PI3K/Akt pathway; Proliferation

1. Introduction

Folate is essential for the development, function and repair of the central nervous system. Folate deficiency and folic acid (FA) therapy have been implicated in the etiology and treatment of human neural tube defects and animal models of neurodegenerative disease [1–4]. FA rescues the proliferation potential of neural precursors in Sp−/− embryos [1]. Further, FA accelerates the proliferation of neural stem cells (NSCs) by a dose-dependent mechanism that depends on DNA methyltransferase (DNMT) [2]. The latter finding suggests that FA-stimulated DNA methylation is involved in the epigenetic regulation of NSC proliferation. The proliferation of these cells is required for development and repair in the central nervous system [3]. However, the genes or pathways that are epigenetically regulated by FA were rarely reported.

The purpose of the present study was to determine if stimulation by FA of NSC proliferation is associated with changes in the DNA methylome and then to identify the salient signaling pathways. The effects of FA and DNMT on methylation profiles in neonatal rat NSCs were assessed by methylated DNA immunoprecipitation-DNA microarray (MeDIP-Chip). We discovered that the methylation profile of PI3K/Akt/CREB was altered profoundly in NSCs that were induced to proliferate by FA. This discovery provides insight into the mechanism by which FA promotes NSC proliferation. Also, since NSC proliferation *in vitro* is a necessary step towards obtaining sufficient NSCs for transplantation therapy to treat neurodegenerative diseases, our discovery may speed the development of NSC-based therapy.

Abbreviations: CGI, CpG island; DMG, differentially methylated gene; DMR, differentially methylated region; DNMT, DNA methyltransferase; FA, folic acid; HCP, high CpG density promoter; LCP, low CpG density promoter; ICP, intermediate CpG density promoter; MTT, methyl thiazolyl tetrazolium; NSC, neural stem cell; QDMR, quantitative differentially methylated region.

☆ Author disclosures: M. Yu, W. Li, S. Luo, Y. Zhang, H. Liu, Y. Gao, X. Wang, J. X. Wilson and G. Huang have no conflicts of interest.

☆☆ This work was supported by grants from the National Natural Science Foundation of China (No. 81072289, 81130053 and 81273056) and Science and Technology Development Project for Universities in Tianjin of China funded by Tianjin Education Commission (No. 20100103).

* Corresponding author. Tel.: +86-22-83336606; fax: +86-22-83336603.
E-mail address: huangguowei@tmu.edu.cn (G. Huang).

[1]M.Y. and W.L. contributed equally to this work.

0955-2863/$ - see front matter © 2014 Elsevier Inc. All rights reserved.
http://dx.doi.org/10.1016/j.jnutbio.2013.12.010

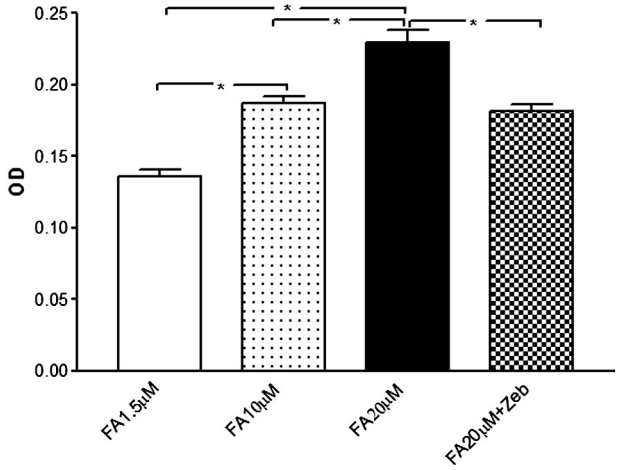

Fig. 1. NSC proliferation increases with FA treated and assessed by MTT assay. *P<.05.

2. Materials and methods

2.1. Cell culture and treatments

The Tianjin Medical University Animal Ethics Committee approved the animal protocols. Pregnant Sprague–Dawley rats were purchased from Beijing Medical Laboratory Animal Co. Ltd (Beijing, China). NSCs were isolated from neonatal (less than 24 h post-natal) Sprague–Dawley rats and cultured as described previously [2]. To assess the effects of FA and DNMT, NSCs were incubated for 48 h with the indicated concentrations of FA and the DNMT inhibitor zebularine. The four treatment groups were FA 1.5 μmol/L (this group was folate deficient and therefore named the D group), FA 10 μmol/L (this group received the normal level of FA supplementation and was named the N group), FA 20 μmol/L (F group) and FA 20 μmol/L plus zebularine 150 μmol/L (Z group).

2.2. Cell proliferation

Cell proliferation was detected by measuring methyl thiazolyl tetrazolium (MTT) reduction, which increases with the number of viable cells. First, NSCs were seeded into 96-well microplate (100 μl/well) treated with indicated concentration of FA for 48 h. Then 10 μl MTT (5 mg/ml) was added to each well and the cells were incubated at 37°C for 4 h. Next, the culture medium was removed and 150 μl DMSO was added to each well. After shaking thoroughly for 10 min, the OD value of each well was read in a microplate reader (Bio-Tek ELX800uv; Bio-Tek Instrument Inc, Winooski, VT, USA) at 570 nm. Data were shown as mean±S.E.M. for each group, based on three independent experiments.

2.3. MeDIP-Chip

Genomic DNA was extracted from 12 cell samples using a DNeasy Blood & Tissue Kit (Qiagen, Fremont, CA). The purified DNA was then quantified and quality assessed by nanodrop ND-1000. Genomic DNA of each sample was sonicated to ~200–1000 bp with a Bioruptor sonicator (Diagenode) on "Low" mode for 10 cycles of 30 s "ON" and 30 s "OFF". The DNA and each sheared DNA were analyzed. Immunoprecipitation of methylated DNA was performed using Biomag magnetic beads coupled to mouse monoclonal antibody against 5-methylcytidine (Diagenode). The genomic DNA (1 μg) was heat denatured at 94°C for 10 min, rapidly cooled on ice and immunoprecipitated with 1 μl primary antibody overnight at 4°C with rocking agitation in 400 μl immunoprecipitation buffer (0.5% bovine serum albumin in phosphate-buffered saline). To recover the immunoprecipitated DNA fragments, 200 μl of anti-mouse IgG magnetic beads was added and incubated for an additional 2 h at 4°C with agitation. After immunoprecipitation, a total of five immunoprecipitation washes were performed with ice-cold immunoprecipitation buffer. Washed beads were resuspended in TE buffer with 0.25% SDS and 0.25 mg/ml proteinase K for 2 h at 65°C and then allowed to cool down to room temperature. MeDIP DNA were purified using Qiagen MinElute columns (Qiagen). MeDIP DNA were amplified using a Whole Genome Amplification kit from Sigma-Aldrich (GenomePlex Complete Whole

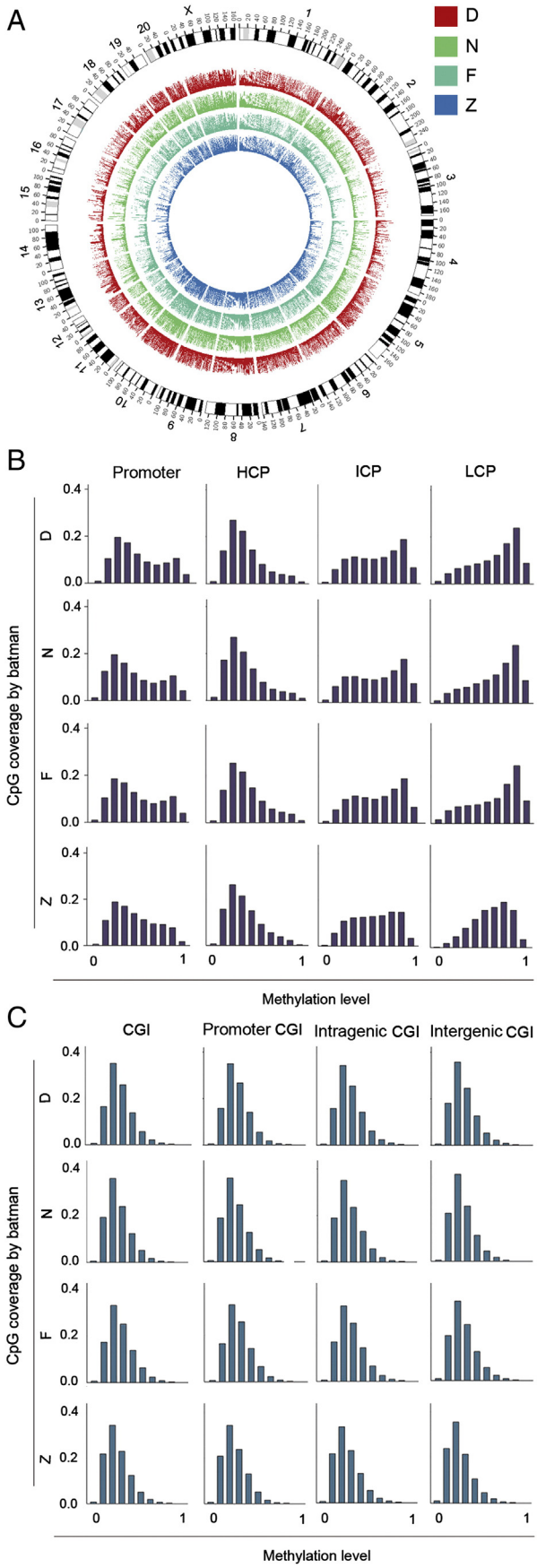

Fig. 2. The DNA methylation levels among four groups. (A) The whole genome-wide DNA methylation levels of D, N, F and Z are represented by Circos histogram. (B) The histograms display the methylation distribution across promoter, HCP, ICP and LCP. (C) The histograms show the methylation distribution across CGI, promoter CGI, intragenic CGI and intergenic CGI.

Genome Amplification kit). The amplified DNA samples were then purified with QIAquick PCR purification kit (Qiagen). The purified DNA was quantified using a nanodrop ND-1000. For DNA labeling, the NimbleGen Dual-Color DNA Labeling Kit was used according to the manufacturer's guideline detailed in the NimbleGen MeDIP-Chip protocol (NimbleGen Systems, Inc, Madison, WI, USA). DNA (1 μg) from each sample was incubated for 10 min at 98°C with 1 OD of Cy5-9mer primer (IP sample) or Cy3-9mer primer (Input sample). Then, 100 pmol of deoxynucleoside triphosphates and 100 U of the Klenow fragment (New England Biolabs, USA) were added, and the mix was incubated at 37°C for 2 h. The reaction was stopped by adding 0.1 volume of 0.5 mol/L EDTA, and the labeled DNA was purified by isopropanol/ethanol precipitation. The total input and immunoprecipitated DNA were labeled with Cy3- and Cy5-labeled random nanomers, respectively, and hybridized to NimbleGen Rat CpG Promoter arrays, which is a single array design containing 15,809 CpG islands (CGIs) and all well-characterized RefSeq promoter regions (from about −1300 bp to +500 bp of the TSSs) totally covered by ~385,000 probes. Scanning was performed with the Axon GenePix 4000B microarray scanner. Raw data were extracted as pair files by NimbleScan software. We perform median-centering, quantile normalization and linear smoothing by Bioconductor packages Ringo, limma and MEDME. After normalization, a normalized $\log_2$-ratio data (IP/Input) was created for each sample. From the normalized $\log_2$-ratio data, a sliding-window peak-finding algorithm provided by NimbleScan v2.5 (Roche-NimbleGen) was applied to find the enriched peaks with specified parameters (sliding window width: 750 bp; mini probes per peak: 2; *P* value minimum cutoff: 2; maximum spacing between nearby probes within peak: 500 bp). After getting the *_peaks.gff files, the identified peaks were mapped to genomic features.

2.4. Identification of differentially methylated regions and differentially methylated genes

Based on methylation profiles [4], we used quantitative differentially methylated region (QDMR) [5] to quantify methylation difference and identify differentially methylated regions (DMRs) from genome-wide methylation profiles among the D, N and F groups as well as between the F and Z groups. QDMR is an entropy-based method for quantification of methylation difference and identification of DMRs and available at http://bioinfo.hrbmu.edu.cn/qdmr/. QDMR is independent of data distribution. The platform-free and species-free nature of QDMR makes it widely used in human and mouse methylation studies. The QDMR entropy ranges from zero for regions differentially methylated in a single sample to a maximum value for regions with uniform methylation levels in all samples considered. The default thresholds (1.659 for two samples and 0.697 for three samples) were used to identify DMRs between the F and Z groups, as well as those among the D, N and F groups. The regions with entropy below the threshold were identified as DMRs. We defined a gene region as the 1300 bp upstream of the TSS to the TTS. For each gene, we calculated the number of DMRs located in its gene region. The more DMRs in the gene region, the more robust is the differential methylation in the gene. To obtain more accurate differentially methylated genes (DMGs), we considered a gene with at least three DMRs as differentially methylated.

2.5. Promoter and CGI classification

Promoters are defined as the [−1300 bp, +500 bp] regions around TSS. Promoter is defined as high CpG density promoter (HCP), which meets GC content ≥0.55 and CpG

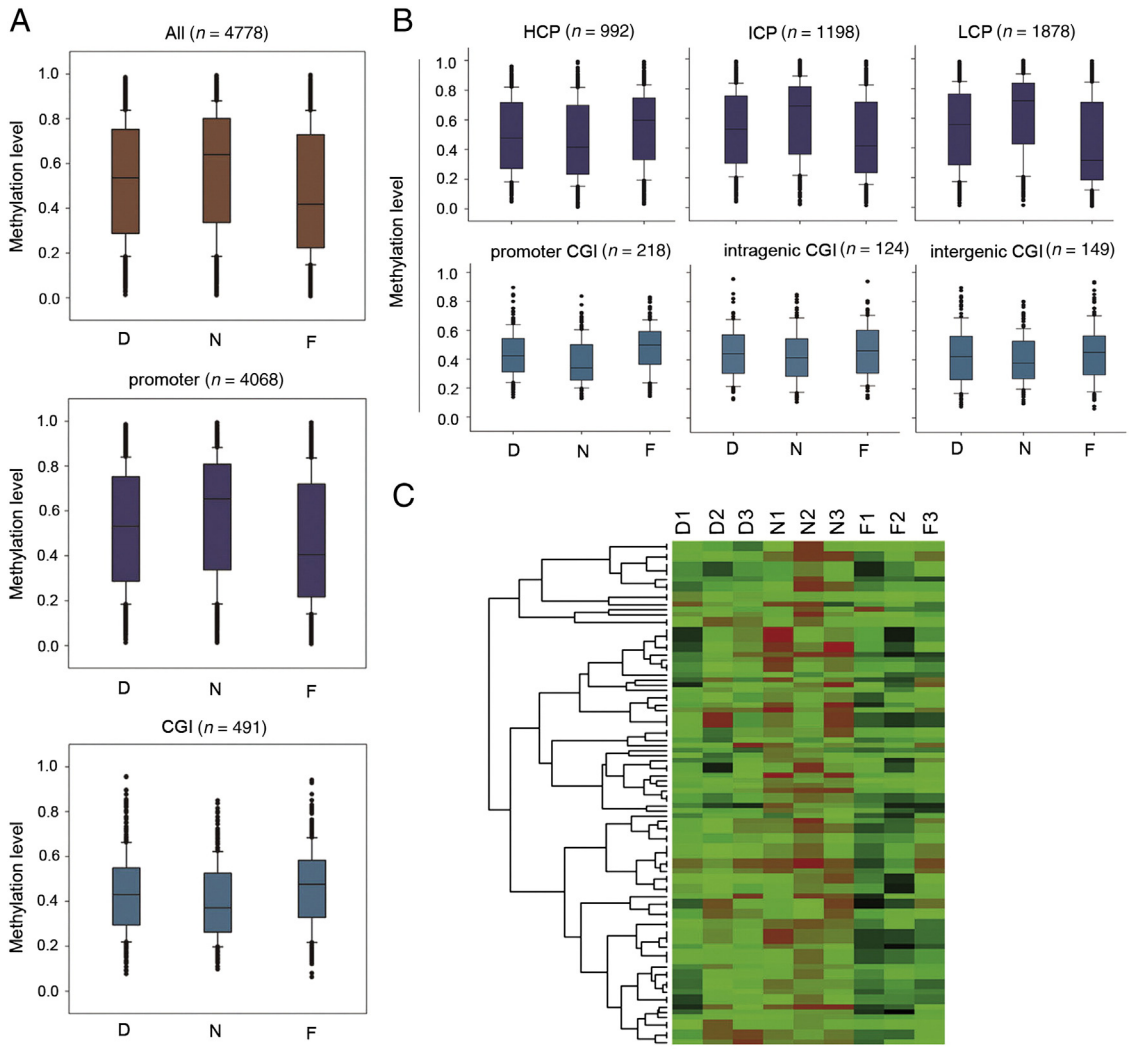

Fig. 3. The DNA methylation distribution of DMRs among D, N and F. (A) The DNA methylation levels of DMRs among D, N and F is illustrated across whole genome-wide, promoters and CGIs. (B) The DNA methylation levels of DMRs located in HCP, ICP, LCP, promoter CGI, intragenic CGI and intergenic CGI. (C) Hierarchical clustering methylation levels of D, N and F replicates and visualized by heat map. Each row represents methylation levels of a single DMR across D, N and F. D1, D2 and D3 refer to three separate MeDIP-Chip assays with 1.5 μmol/L FA-treated NSCs; N1, N2 and N3 refer to three separate MeDIP-Chip assays with 10 μmol/L FA-treated NSCs; F1, F2 and F3 refer to three separate MeDIP-Chip assays with 20 μmol/L FA-treated NSCs.

O/E ≥0.6 in a 500-bp window within −700 bp to +200 bp around TSS. Promoter is defined as low CpG density promoter (LCP), which has not met CpG O/E more than 0.4 in any 500-bp window. The remaining promoter is defined as intermediate CpG density promoter (ICP). CGI is defined as promoter CGI with its midpoint located in −10 kb to TSS. CGI is defined as intragenic CGI with its midpoint located in the TSS to the TTS. The remaining CGI is defined as intergenic CGI.

2.6. Pathway analysis

Pathway analysis was used to find out the significant pathway of the differential methylated genes. Pathway annotations of genes were downloaded from KEGG [6] (http://www.genome.jp/kegg/). A Fisher exact test was used to find the significant enrichment pathway. The resulting P values were adjusted using the BH FDR algorithm [7]. Pathway categories with a FDR<0.05 were reported. The enrichment was given by the following: enrichment=$(n_g/n_a)/(N_g/N_a)$, where n_g is the number of differential genes within the particular pathway, n_a is the total number of genes within the same pathway, N_g is the number of differential genes that have at least one pathway annotation and N_a is the number of genes that have at least one pathway annotation in the entire microarray.

2.7. Pathway map

The KEGG database was used to reveal the gene network of DMGs [8,9]. The KEGG pathway map is a molecular interaction network diagram represented in terms of the KEGG Otology groups so that experimental evidence in a specific organism can be generalized to other organisms through genomic information.

3. Results

3.1. Effect of FA on NSC proliferation

FA stimulated NSC proliferation dose dependently at 10 and 20 μmol/L (Fig. 1). With the increasing of FA, NSC proliferation is increased (P<.05). The DNMT inhibitor zebularine counteracted the proliferative effect of FA (Fig. 1). Thus the stimulatory effect of FA on NSC proliferation may be mediated by DNA methylation.

3.2. Effects of FA and DNMT on DNA methylation maps

The whole genome-wide DNA methylation maps of groups D (1.5 μmol/L FA), N (10 μmol/L FA), F (20 μmol/L FA) and Z (20 μmol/L FA plus 150 μmol/L zebularine) were depicted in Fig. 2A by Circos [10] (Fig. 2A). The DNA methylation levels among the D, N and F groups showed significant difference (Kruskal–Wallis test, P<.001). The Mann–Whitney Rank Sum test between F and Z groups also demonstrated significant difference (P<.001).

We also display the patterns of DNA methylation in promoters and CGIs in the genome. In group D, N and F, the DNA methylation levels of promoters and ICPs had bimodal distributions (Fig. 2B) but CGIs displayed low methylation levels and unimodal distribution (Fig. 2C), which is consistent with previous report. Also in groups D, N and F, most HCPs were unmethylated while most LCPs showed the opposite. Similarly, the majority of CGIs were unmethylated regardless of their genome positions. All in all, although the FA concentration is varying among D, N and F, the DNA methylation distribution is similar in different functional genomic regions.

Compared to group F, group Z had similar DNA methylation levels in high CpG density genome regions (HCPs, CGIs and CGI categories) but different levels in the comparatively low CpG density regions (ICPs and LCPs) (Fig. 2B and C), which indicate that methyl blockers mostly affect the methylation of low CpG density genomic regions while they have little effect with high CpG density regions.

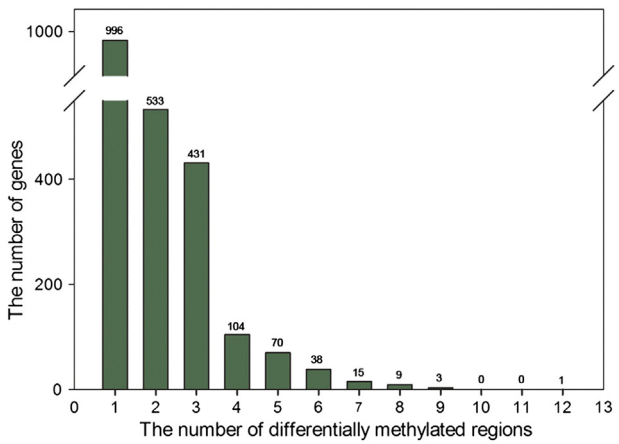

Fig. 4. The DMG number varies following the number of DMRs across D, N and F. Nearly half of genes just have one DMR.

3.3. Dose-dependent effects of FA on DMRs

Moreover, the DMRs among D, N and F groups with different effects of FA are investigated. Fig. 3A shows the methylation distributions of DMRs in whole genome-wide, promoters and CGIs. The methylation levels of N group are the highest, whereas F group is the lowest in the whole genome-wide and promoters. However, the

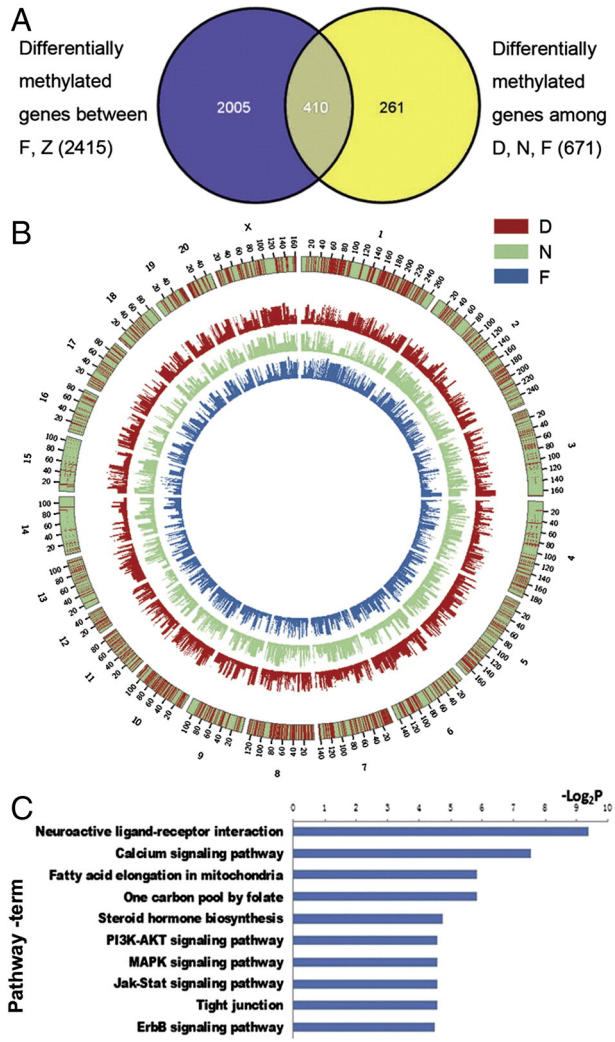

Fig. 5. DMGs and pathway analysis. (A) The figure shows the number of DMGs between F and Z and the number of DMGs across D, N and F. (B) The methylation levels of DMGs across D, N and F. The most outside ring represents the genome annotation and the red regions in the ring represent genes. The inner three rings represent the methylation levels of D, N and F, respectively, using Circos histogram. (C) Pathway analysis of DMGs was performed to find out the significant pathway of the differential genes.

methylation distributions of CGIs have a reversed result compared to whole genome-wide and promoters.

Groups D, N and F were also compared according to the DNA methylation levels of DMRs located in HCPs, ICPs, promoter CGIs, intragenic CGIs and intergenic CGIs (Fig. 3B). The methylation distributions in HCPs among D, N and F groups were different from the ICPs and the LCPs, while they were the same with CGIs. Moreover, three categories of CGIs displayed the same methylation distribution with whole CGIs (Fig. 3B). Overall, the methylation level distribution in high CpG density genome regions is consistent with what Fig. 2 shows.

Finally, we selected the top 100 DMRs for further study used cluster analysis. Fig. 3C shows significant difference of methylation levels across three groups and consistent methylation levels within group. It suggests that the DNA methylation is a dose-dependent effect of FA.

3.4. Analysis of the genes with DMRs

We next mapped DMRs to genome according to the identified DMRs across D, N and F. Fig. 4 shows nearly half of genes with more than one DMR in its gene region. To improve confidence, we choose the genes containing three or more DMRs as DMG (see details in method). There are 671 genes identified as DMGs across D, N and F groups (Fig. 5A). The difference of the 671 genes methylation levels across D, N and F are shown in Fig. 5B. Furthermore, pathway analysis was performed for these genes by KEGG. They are enriched in neuroactive ligand–receptor interaction, calcium signaling pathway, PI3K/Akt, MAPK signaling pathway and one carbon pool by folate and Jak-STAT signaling pathway (Fig. 5C). It suggests that these DMGs play an important role in response to folate stimulation.

In addition, 2415 DMGs identified between F and Z have significant effect on the methyl blockers of genes (Fig. 5A). To further analyze the genes affected by folate, we investigated the 410 overlap genes between 671 genes and 2415 genes (Fig. 5A). Moreover, we performed pathway analysis for these 410 genes and the enriched terms are almost the same as the previous 671 genes.

3.5. Gene network of DMGs

Functional network analysis of DMGs generated subnetworks based on their functional annotation and known molecular interactions, which were composed of 27 focus genes (Fig. 6, marked with yellow) and 23 D, N and F DMGs (marked with red). The main subnetworks included neuroactive ligand–receptor interaction, Jak-STAT signaling pathway, steroid biosynthesis, fatty acid elongation, PI3K/Akt, MAPK signaling pathway and cytokine–cytokine receptor interaction. Akt3 acted as a hub by interacting with genes encoding the neurotrophin signaling pathway, PI3K/Akt, mTOR signaling pathway, Jak-STAT, tight junctions and focal adhesion.

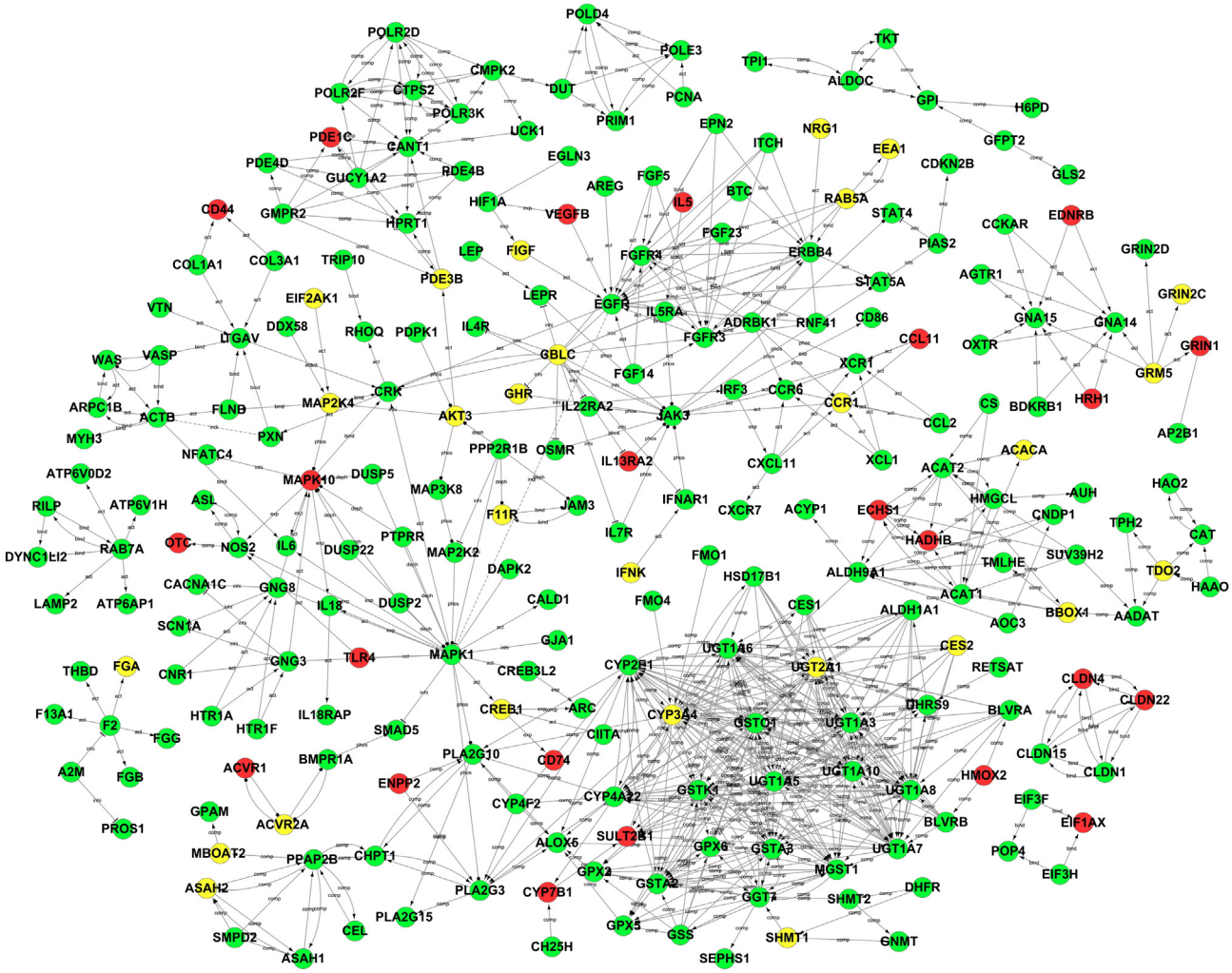

Fig. 6. Gene Act Network of DMGs. It is based on the analysis of the KEGG database to build the network of genes according to the relationship among the differential genes in the database. Marked with red correspond to DMGs across D, N and F. The green ones correspond to DMGs between F and Z. The yellow ones correspond to the overlap genes between the above two groups.

3.6. DMGs converge to PI3K/Akt signaling pathway

Based on the pathway analysis and the number of DMRs in DMGs, the PI3K/Akt pathway was highlighted. The 14 DMGs across the D, N and F groups included Akt (Akt3), CREB (Creb1), CDK (Cdk2, Cdk5 and Cdkal1_predicted), cytokines (Il1f6_predicted, Il5, Il1f5_predicted and Tnfaip812), cytokineR (Il13ra2, Tnfrs10b_predicted and Tnfrsf4) and TLR (Tlr4 and Tlr3) (Fig. 7). Four nodes of the PI3K/Akt pathway, namely, Akt, CREB, cytokineR and CDK, belonged to the overlap DMGs group across D, N, F and Z (Fig. 8). Thus FA modifies the methylation profile of the PI3K/Akt pathway.

4. Discussion

4.1. FA-induced changes in global DNA methylation profile

The genome-wide DNA methylation analysis of D, N, F and Z groups displayed quite different DNA methylation distribution profiles, which implies that FA does impact DNMT-mediated DNA methylation in proliferating NSCs. The DNA methylation levels of promoters and ICPs had bimodal distributions (Fig. 2B) but CGIs displayed low methylation levels and unimodal distribution (Fig. 2C) in D, N and F groups, which is consistent with the previous study [11–13]. By comparing the methylation distribution maps across HCP, ICP and LCP, it is clear that the effects on DNA methylation are localized mostly to LCP. Generally, LCP is considered to be associated with tissue-specific genes [11]. Thus FA only affects some specific genes or regions rather than the overall DNA methylation level.

The methylation distribution of DMRs showed most DMRs (4068/4778) located in promoters and a considerable amount (1879/4068) of promoter DMRs located in LCPs. DMRs in ICP and LCP of D and F groups both exhibited hypomethylation compared to N group, while the inverse was observed in HCP. The data imply that either FA deficiency or supplementation may decrease methylation levels in LCP promoters of some genes.

4.2. FA stimulates NSC proliferation by altering methylation levels in PI3K/Akt/CREB

The present study revealed a novel role of PI3K/Akt/CREB pathway in FA-stimulated NSC proliferation. We showed, apparently for the first time, that DNA methylation levels in key components of PI3K/Akt/CREB, including Akt, CREB and CDK, were significantly altered with FA variations. PI3K/Akt is associated with anti-apoptotic and survival functions [14] and transduces mitogenic signals that drive proliferation and inhibit differentiation of adult neural progenitors [15]. PI3K activity has been implicated in regulation of proliferation of embryonic NSC [16]. Akt has also been shown to play a role in self-renewal of embryonic stem cells and fetal neural progenitors [17–19]. Additionally, Akt3$^{-/-}$ deficient mice have reduced brain size and weight that indicated its crucial role in the development of the central nervous system [20]. PI3K/Akt has a number of downstream effectors including mTOR, CREB, CDK and so on. CREB is a transcription factor that induces the transcription of more than 100 genes under the control of cAMP response element [21]. CREB is involved in regulating adult neural hippocampal progenitor proliferation and differentiation [15]. CREB can be activated by Akt via direct phosphorylation and is generally considered that it is positively regulated by PI3K/Akt pathway in PC12 cells, neonatal cardiomyocytes and striatal neurons [22–25].

In conclusion, FA alters DNA methylation profiles profoundly while increasing NSC proliferation. FA affects DNA methylation at specific loci, rather than across the genome, because DMRs pooled to LCPs. DMGs converge to PI3K/Akt/CREB and most of these genes contained more than three DMRs. These findings are consistent with the idea that that FA stimulates NSC proliferation by modifying DNA methylation levels of key components of PI3K/Akt/CREB.

Symbols in pathway map	DMGs in this study	Number of DMRs	The methylation level in D	The methylation level in N	The methylation level in F	The methylation level in Z
AKT	Akt3	3	0.26	0.61	0.21	0.72
CREB	Creb1	9	0.37	0.51	0.28	0.33
CDK	Cdk2	5	0.27	0.25	0.42	0.23
	Cdkal1_predicted	4	0.33	0.18	0.55	0.29
	Cdk5	3	0.59	0.45	0.58	0.49
Cytokine	Il1f6_predicted	3	0.43	0.48	0.37	0.42
	Il5	3	0.82	0.72	0.75	0.67
	Il1f5_predicted	2	0.59	0.48	0.83	0.57
	Tnfaip8l2	3	0.77	0.67	0.76	0.67
CytokineR	Il13ra2	3	0.64	0.82	0.13	0.35
TLR	Tlr4	3	0.76	0.84	0.68	0.61

Fig. 7. Methylation variations of DMGs in the PI3K/Akt/CREB signaling pathway.

Acknowledgements

The authors' responsibilities were as follows: G.H., developed and designed the concept; M.Y., W.L., S.L., H.L., Y.G. and X.W., designed and conducted the research; M.Y. and Y.Z., performed the statistical analysis; W.L., M.Y., Y.Z. and J.X.W., drafted the manuscript; and M.Y., W.L. and G.H. had primary responsibility for the final content. All authors read and approved the final manuscript. None of the authors declared a conflict of interest.

References

[1] Ichi S, Costa FF, Bischof JM, Nakazaki H, Shen YW, Boshnjaku V, et al. Folic acid remodels chromatin on Hes1 and Neurog2 promoters during caudal neural tube development. J Biol Chem 2010;285:36922–32.
[2] Li W, Yu M, Luo S, Liu H, Gao Y, Wilson JX, et al. DNA methyltransferase mediates dose-dependent stimulation of neural stem cell proliferation by folate. The Journal of nutritional biochemistry 2013;24:1295–301.
[3] Zhang X, Huang G, Liu H, Chang H, Wilson JX. Folic acid enhances Notch signaling, hippocampal neurogenesis, and cognitive function in a rat model of cerebral ischemia. Nutr Neurosci 2012;15:55–61.
[4] Down TA, Rakyan VK, Turner DJ, Flicek P, Li H, Kulesha E, et al. A Bayesian deconvolution strategy for immunoprecipitation-based DNA methylome analysis. Nat Biotechnol 2008;26:779–85.
[5] Zhang Y, Liu H, Lv J, Xiao X, Zhu J, Liu X, et al. QDMR: a quantitative method for identification of differentially methylated regions by entropy. Nucleic Acids Research 2011;39:e58-e.
[6] Kanehisa M, Goto S, Sato Y, Furumichi M, Tanabe M. KEGG for integration and interpretation of large-scale molecular data sets. Nucleic Acids Res 2012;40:D109–14.
[7] Klipper-Aurbach Y, Wasserman M, Braunspiegel-Weintrob N, Borstein D, Peleg S, Assa S, et al. Mathematical formulae for the prediction of the residual beta cell function during the first two years of disease in children and adolescents with insulin-dependent diabetes mellitus. Med Hypotheses 1995;45:486–90.
[8] Jansen R, Greenbaum D, Gerstein M. Relating whole-genome expression data with protein–protein interactions. Genome Res 2002;12:37–46.
[9] Zhang JD, Wiemann S. KEGGgraph: a graph approach to KEGG PATHWAY in R and bioconductor. Bioinformatics 2009;25:1470–1.

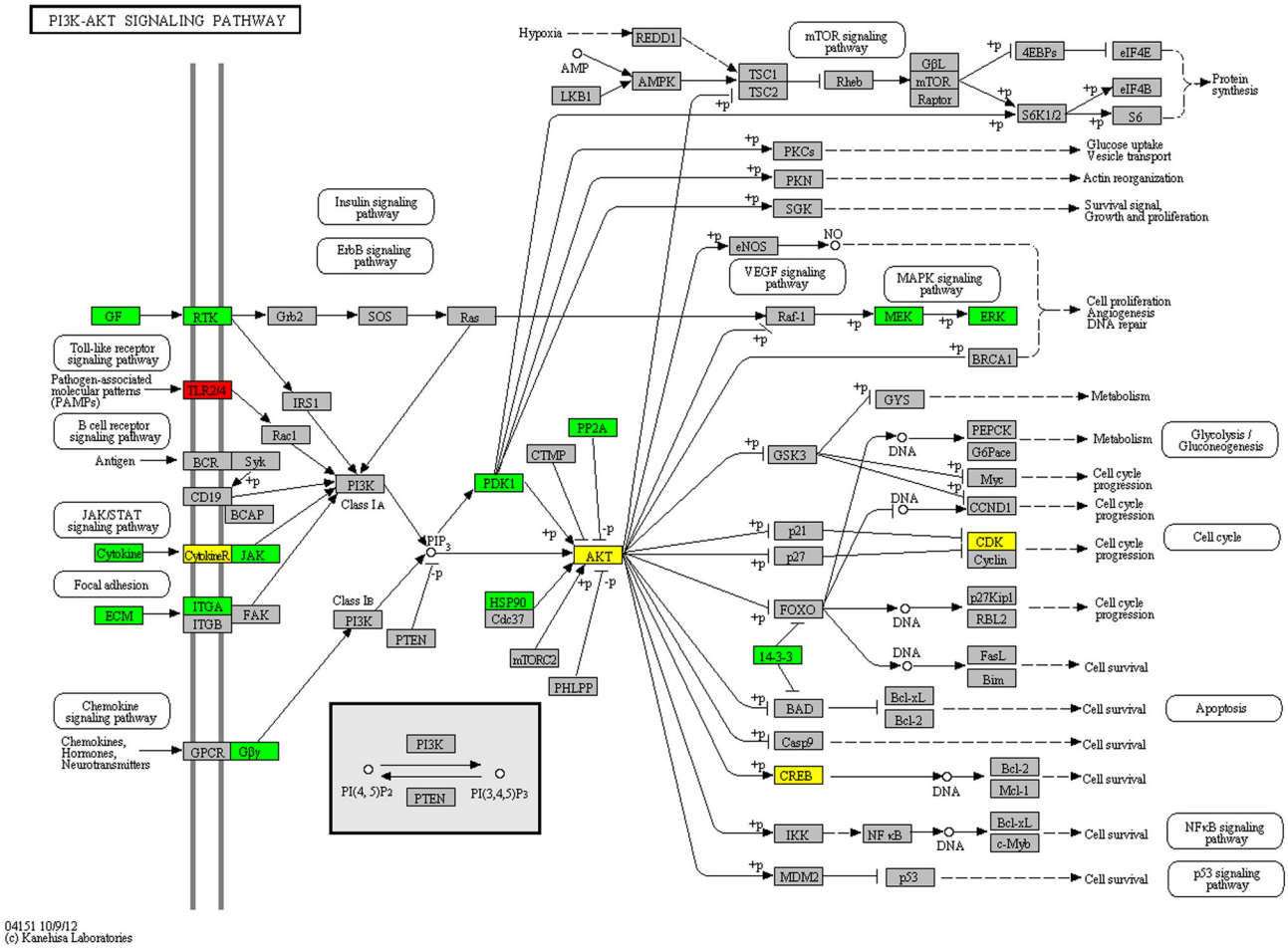

Fig. 8. DMGs in PI3K/Akt signaling pathway. FA-induced DMGs were highlighted in PI3K/Akt signaling pathway. The red, green and yellow correspond to DMGs across D, N and F; DMGs between F and Z and the overlap genes, respectively.

[10] Krzywinski M, Schein J, Birol I, Connors J, Gascoyne R, Horsman D, et al. Circos: an information aesthetic for comparative genomics. Genome Res 2009;19:1639–45.
[11] Meissner A, Mikkelsen TS, Gu H, Wernig M, Hanna J, Sivachenko A, et al. Genome-scale DNA methylation maps of pluripotent and differentiated cells. Nature 2008;454:766–70.
[12] Antequera F, Bird A. Number of CpG islands and genes in human and mouse. Proc Natl Acad Sci U S A 1993;90:11995–9.
[13] Cedar H, Bergman Y. Linking DNA methylation and histone modification: patterns and paradigms. Nat Rev Genet 2009;10:295–304.
[14] Datta SR, Brunet A, Greenberg ME. Cellular survival: a play in three Akts. Genes Dev 1999;13:2905–27.
[15] Peltier J, O'Neill A, Schaffer DV. PI3K/Akt and CREB regulate adult neural hippocampal progenitor proliferation and differentiation. Dev Neurobiol 2007;67:1348–61.
[16] Groszer M, Erickson R, Scripture-Adams DD, Dougherty JD, Le Belle J, Zack JA, et al. PTEN negatively regulates neural stem cell self-renewal by modulating G0–G1 cell cycle entry. Proc Natl Acad Sci U S A 2006;103:111–6.
[17] Paling NR, Wheadon H, Bone HK, Welham MJ. Regulation of embryonic stem cell self-renewal by phosphoinositide 3-kinase-dependent signaling. J Biol Chem 2004;279:48063–70.
[18] Watanabe S, Umehara H, Murayama K, Okabe M, Kimura T, Nakano T. Activation of Akt signaling is sufficient to maintain pluripotency in mouse and primate embryonic stem cells. Oncogene 2006;25:2697–707.
[19] Sinor AD, Lillien L. Akt-1 expression level regulates CNS precursors. J Neurosci 2004;24:8531–41.
[20] Tschopp O, Yang ZZ, Brodbeck D, Dummler BA, Hemmings-Mieszczak M, Watanabe T, et al. Essential role of protein kinase B gamma (PKB gamma/Akt3) in postnatal brain development but not in glucose homeostasis. Development 2005;132:2943–54.
[21] Mayr B, Montminy M. Transcriptional regulation by the phosphorylation-dependent factor CREB. Nat Rev Molec Cell Biol 2001;2:599–609.
[22] Du K, Montminy M. CREB is a regulatory target for the protein kinase Akt/PKB. J Biol Chem 1998;273:32377–9.
[23] Pugazhenthi S, Nesterova A, Sable C, Heidenreich KA, Boxer LM, Heasley LE, et al. Akt/protein kinase B up-regulates Bcl-2 expression through cAMP-response element-binding protein. J Biol Chem 2000;275:10761–6.
[24] Mehrhof FB, Muller FU, Bergmann MW, Li P, Wang Y, Schmitz W, et al. In cardiomyocyte hypoxia, insulin-like growth factor-I-induced antiapoptotic signaling requires phosphatidylinositol-3-OH-kinase-dependent and mitogen-activated protein kinase-dependent activation of the transcription factor cAMP response element-binding protein. Circulation 2001;104:2088–94.
[25] Brami-Cherrier K, Valjent E, Garcia M, Pages C, Hipskind RA, Caboche J. Dopamine induces a PI3-kinase-independent activation of Akt in striatal neurons: a new route to cAMP response element-binding protein phosphorylation. J Neurosci 2002;22:8911–21.